Supporting Information

Synergistic residual strain regulation and defect passivation in high-efficiency inverted perovskite solar cells

Yufei Guo,[†a] Shiqiong Wang,[†a] Jiankai Zhang,[*a] Wenyi Wu,[a] Yuning Zhang,[*b] Chengwen Huang[c] and Hai Zhou[*a]

[a]*International School of Microelectronics, Dongguan University of Technology, Dongguan 523808, Guangdong, China*

[b]*School of Physics and Optoelectronics, South China University of Technology, Guangzhou 510640, Guangdong, China*

[c]*School of Optoelectronic Engineering, Guilin University of Electronic Science and Technology, Guilin 541004, Guangxi, China*

[†]These authors contributed equally to this work.

*Corresponding author E-mail address: jkzhang@dgut.edu.cn (J. Zhang), yuningzhang10@163.com (Y. Zhang), hizhou@dgut.edu.cn (H. Zhou).

Experimental Section

Materials: Etching indium tin oxide (ITO)

Device fabrication: The etched ITO substrates were sequentially cleansed with deionized water, acetone, and isopropanol, each for 15 minutes, followed by drying for 12 hours. Subsequently, the dried ITO surfaces were treated with oxygen plasma for 20 minutes to eliminate organic residues and enhance surface wettability. A film of either MeO-2PACZ or F-PhPACZ was spin-coated onto the ITO substrates at 4000 rpm for 30 s, followed by thermal annealing at 100 °C for 10 min in a nitrogen-filled glovebox. To prepare the $FA_{0.95}Cs_{0.05}PbI_3$ perovskite precursor, 201.2 mg of FAI, 33.8 mg of CsI, 2 mg of TIBBP (or without) and 629.3 mg of PbI_2 were dissolved in a mixed solvent of DMF and DMSO in a 4:1 volume ratio. The resulting solution was then spin-coated onto the pretreated ITO substrates (4000 rpm, 30 s). At the 20 s, 180 μL of CB was swiftly dripped onto the spinning film as an anti-solvent. The coated films were subsequently annealed at 100 °C for 20 min. A 50 μL solution of PEAI (1.5 mg/mL) was spin-coated onto the perovskite layer (3000 rpm, 30 s) to form a passivation layer. It was followed by spin-coating 25 μL of $PC_{61}BM$ (20 mg/mL in CB) at 4000 rpm for 30 s. Subsequently, 40 μL of BCP (0.5 mg mL–1 in IPA) was dynamically spin-coated at 4000 rpm for 30 s. Finally, a silver electrode with a thickness of 80 nm was deposited via thermal evaporation. The effective area defined by the shadow mask was 0.08 cm^2. In addition, for the fabrication of pure hole-transport devices, the Spiro-OMeTAD solution was spin-coated onto the perovskite layer at 4000 rpm for 40 s.

Characterizations: Fourier transform infrared (FTIR) spectra were performed on a Thermo Scientific Nicolet iS50 instrument. The X-ray diffraction (XRD) curves were measured on a Bruker Discovery D8 diffractometer using Cu-Kα radiation (λ=1.54 Å). The morphological characteristics of the perovskite thin films and material were recorded via field emission scanning electron microscopy (SEM, Hitachi S4700). The atomic force microscope (AFM) measurement was performed on the Multimode 8 AFM from Bruker. X-ray photoelectron spectroscopy (XPS) was recorded on the Thermo Scientific Escalab 250Xi instrument equipped with Mg-Kα source to expose

chemical bonds and energy level status. The UV–Vis DRS spectra was executed on an ocean optics spectrum testing system with a DH-2000-BAL UV–VIS–NIR light source. Photoluminescence (PL) and transient fluorescence decay spectra of the films were characterized by performing a Laser405-1HS illuminant and an FLS920 from Edinburgh Instruments Ltd./UK. The current density-voltage (*J-V*) curves and space charge limited current (SCLC) curves were monitored via a Keithley 2400 source meter equipped with a simulated AM 1.5 G solar system (irradiance of 100 $mW \cdot cm^{-2}$). The external quantum efficiency (EQE) was obtained on an SRF50 system with a with wavelength range of 300-900 nm.

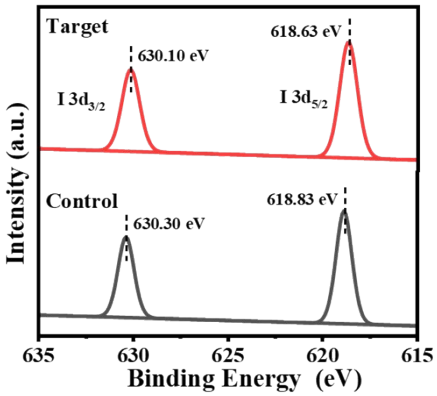

Fig. S1 I 3d core-level for the control and target perovskite films.

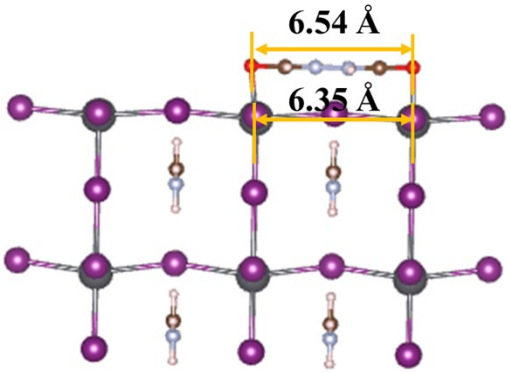

Fig. S2 The length of DFH molecule and the lattice spacing of $FAPbI_3$ perovskite.

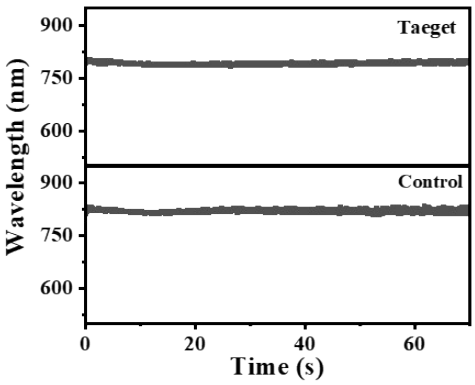

Fig. S3 Corresponding PL peak position extracted from in-situ PL spectra of the control and target perovskite films.

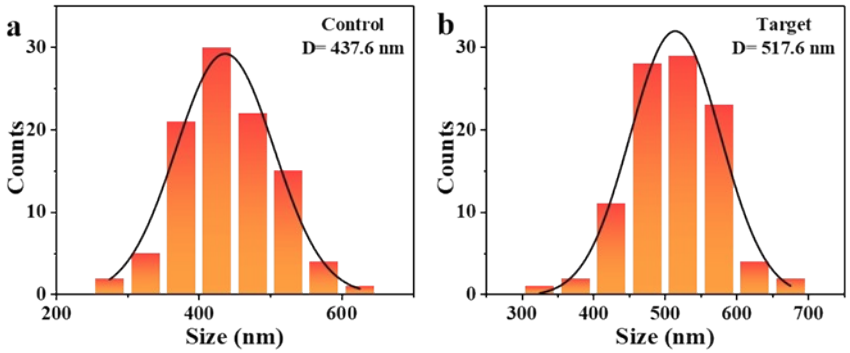

Fig. S4 The grain size distribution of the control and target perovskite films.

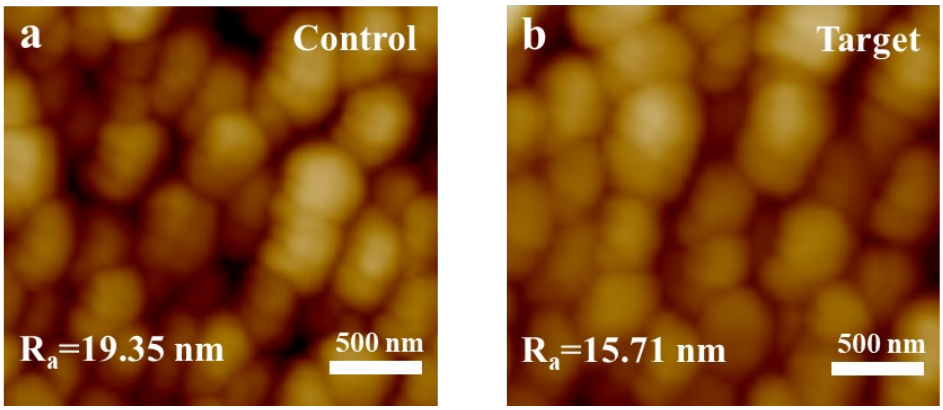

Fig. S5 Top view AFM images of the control and target perovskite films.

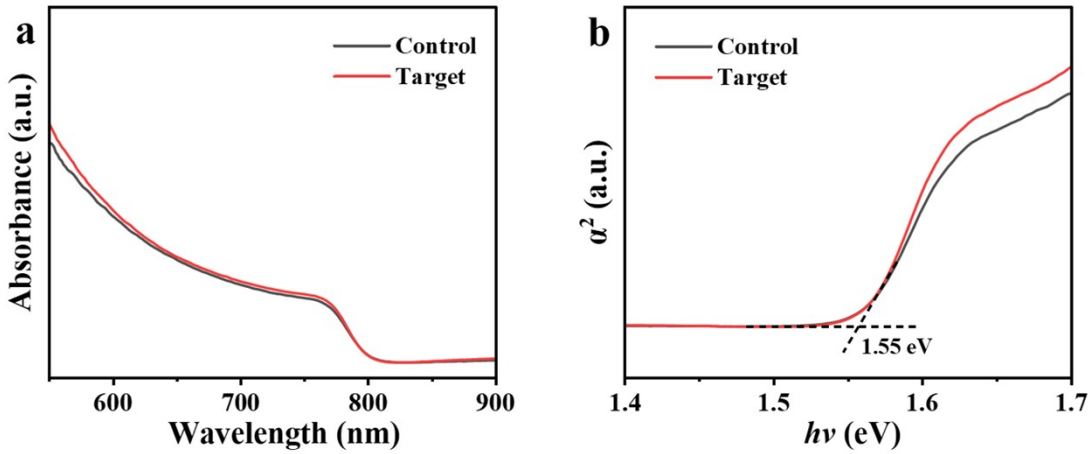

Fig. S6 The absorbance spectra (a) and optical bandgap (b) measurements of the control and target perovskite films.

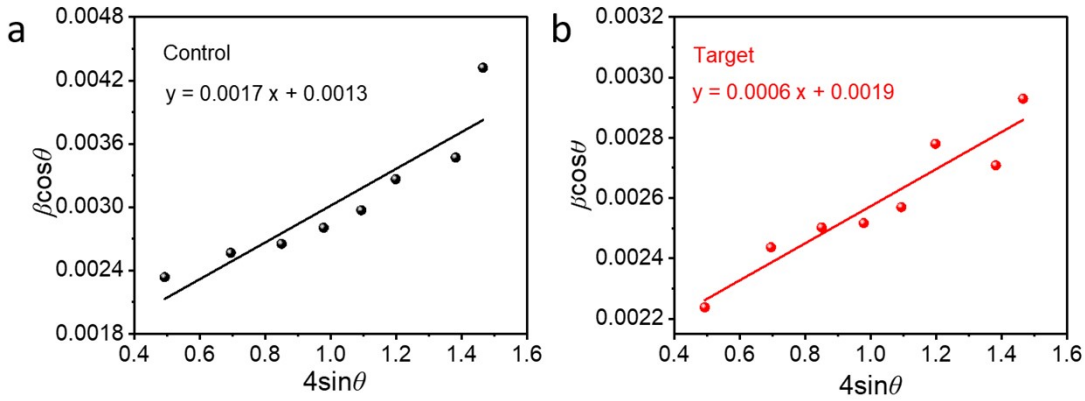

Fig. S7 The plots of βcosθ vs 4sinθ of the control and target films.

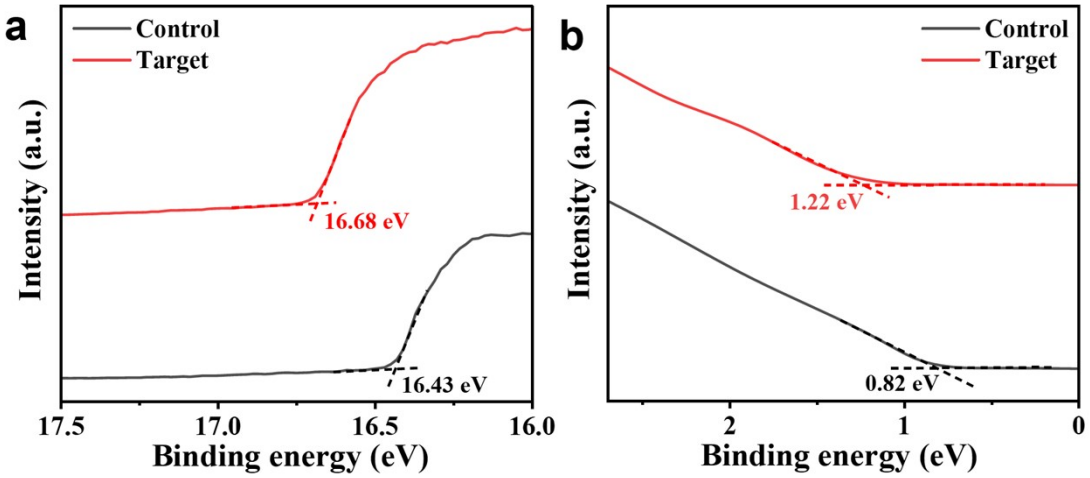

Fig. S8 UPS secondary electron cutoff (a) and onset (b) binding energies of the control and target perovskite films.

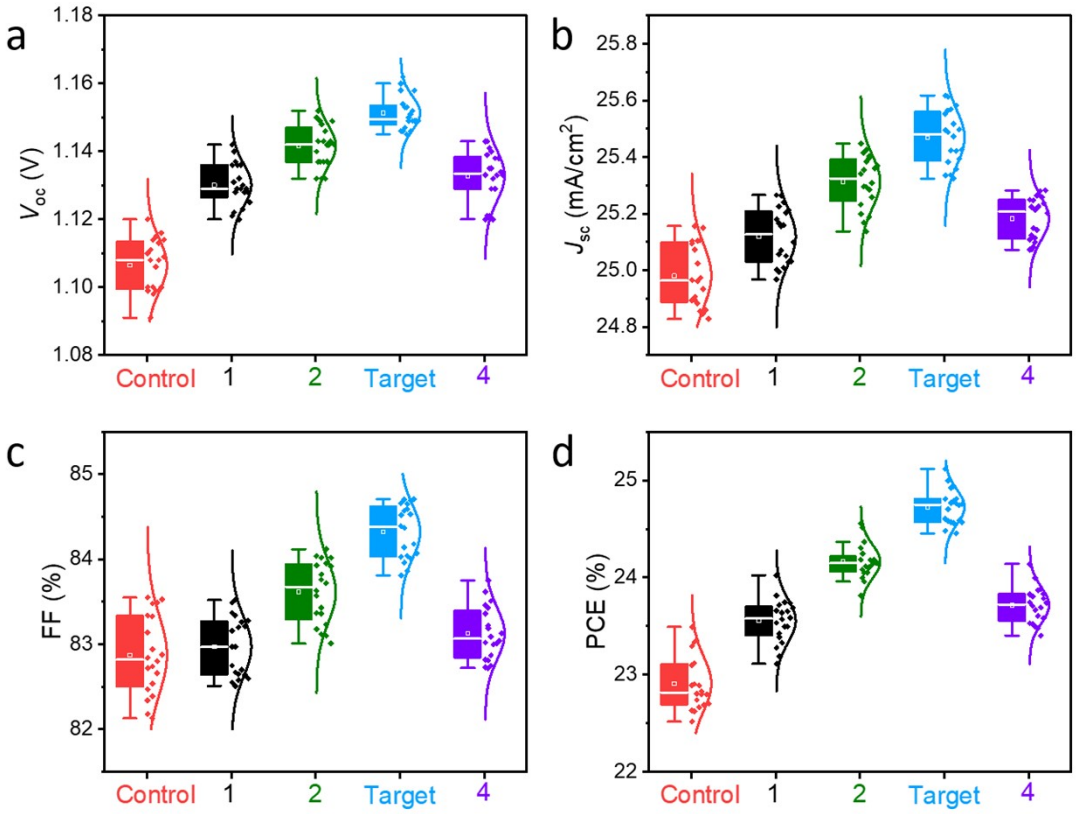

Fig. S9 The performance statistics of PSCs.

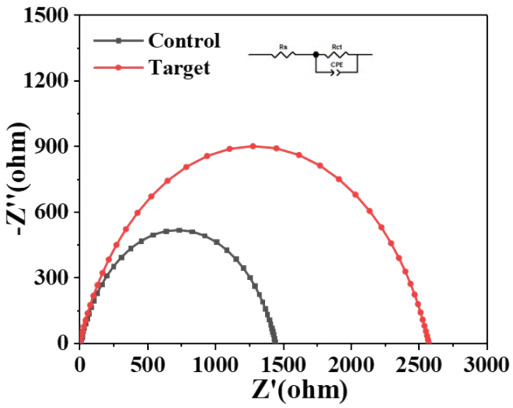

Fig. S10 Nyquist plots of the PSCs.

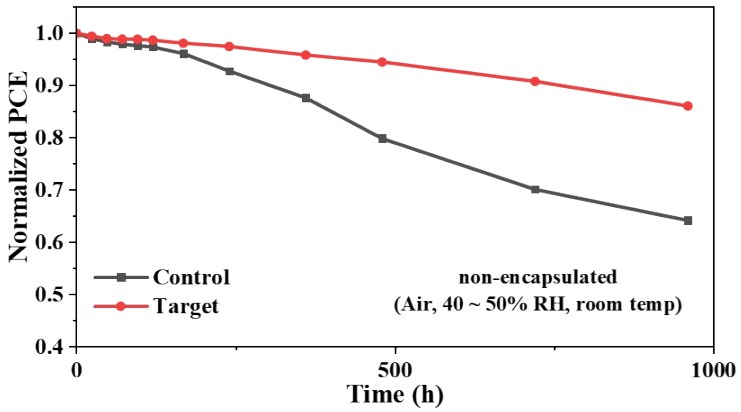

Fig. S11 Moisture stability under a relative humidity (RH) of 40−50% at room temp in air.

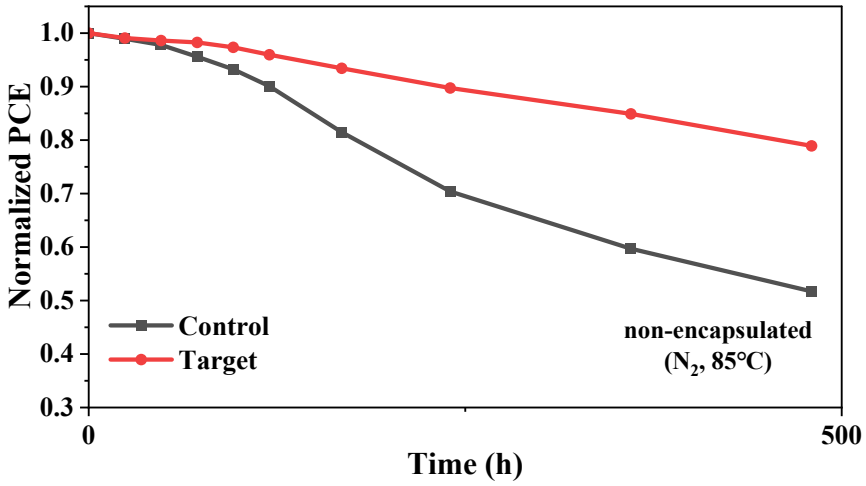

Fig. S12 The thermal stability of the devices at 85 °C in N_2.

Table S1 Summary of bi-exponential fitting results of the TRPL spectra.

Samples	A_1 (%)	τ_1 (ns)	A_2 (%)	τ_2 (ns)	τ_{ave} (ns)
Control	22.14	14.88	77.86	386.37	382.35
Target	29.92	13.42	70.08	281.51	276.16

Table S2 The photovoltaic parameters of the champion PSCs modified with different concentrations of DFH.

Concentrations	J_{sc} (mA/cm^2)	V_{oc} (V)	FF (%)	PCE (%)
Control	25.10	1.12	83.55	23.49
1	25.24	1.14	83.49	24.02
2	25.39	1.15	84.12	24.56
Target	25.57	1.16	84.70	25.12
4	25.28	1.14	83.75	24.14

Table S3 The photovoltaic parameters of the control and target PSCs under different scanning directions.

Scan direction	J_{sc} (mA/cm^2)	V_{oc} (V)	FF (%)	PCE (%)
Control-F	25.10	1.12	83.55	23.49
Control-R	24.75	1.11	83.27	22.88
Target-F	25.57	1.16	84.70	25.12
Target-R	25.44	1.16	84.50	24.94